ELSEVIER

Chemical Geology 161 (1999) 181–198

CHEMICAL GEOLOGY
INCLUDING
ISOTOPE GEOSCIENCE

www.elsevier.com/locate/chemgeo

Interpreting carbon-isotope excursions: carbonates and organic matter

Lee R. Kump *, Michael A. Arthur

Department of Geosciences and Earth System Science Center, The Pennsylvania State University, University Park, PA 16802, USA

Received 11 February 1998; accepted 16 October 1998

Abstract

Variations in the carbon isotopic compositions of marine carbonate and organic carbon provide a record of changes in the fraction of organic carbon buried through time and may provide clues to changes in rates of weathering and sources of organic carbon. Paired carbonate and organic carbon isotope determinations provide a possibility of interpreting not only changes in the global carbon cycle through time, but changes in atmospheric pCO_2 as well. Interpretations of these types of data are typically rather qualitative; a quantitative basis is required to develop a better understanding of changes in the carbon cycle. For this purpose, we employ a simple model of the global carbon cycle which is subjected to a number of different perturbations, each lasting 500 ky, i.e., much longer than the residence times of carbon and phosphorus in the ocean–atmosphere system. In addition to standard considerations of carbon mass and isotopic fluxes to the ocean–atmosphere system from weathering and volcanism and fluxes of organic carbon and carbonate–carbon to sediments, the model incorporates sensitivity of the photosynthetic carbon isotope effect to changes in pCO_2. The inclusion of this parameter leads to unexpected carbon isotope responses to forcing that causes increased rates of organic carbon burial. A series of simple to more complex simulations illustrates the significant effects of varying differences between the carbon isotopic composition of sedimented carbonate and organic carbon (Δ_B). With constant Δ_B a 50% increase in organic carbon burial produces a parallel increase in carbonate and organic carbon isotopic compositions. However, the same simulation with Δ_B responsive to pCO_2 changes produces an initial parallel $\delta^{13}C$ increase, but this is followed by an even greater ^{13}C-enrichment in organic carbon because pCO_2 falls in response to increased organic carbon burial. The counterintuitive overall result of the enhanced organic carbon burial event is that the carbonate carbon isotopic composition actually decreases because of the more substantial increase in $\delta^{13}C_{org}$. In addition, we illustrate the effects on carbon isotopic compositions of the oceanic inorganic carbon reservoir and buried organic matter of a 50% increase in volcanic CO_2 outgassing, a 50% increase in weathering rate (with coupled phosphate and riverine carbon flux responses), a 50% decrease in shale-associated organic carbon weathering, a 50% decrease in silicate weathering rate, and the possible effects of the rise in abundance of C_4 plants in the late Miocene to Recent. We compare the model simulated carbon isotopic responses for some of these experiments to paired carbonate- and organic-carbon records to illustrate how these records might be interpreted in light of the model response.

Keywords: Carbon-13; Isotope excursions; Modeling; Biogeochemical cycles; Organic carbon; Marine geochemistry

* Corresponding author. E-mail: kump@geosc.psu.edu

0009-2541/99/$ - see front matter
PII: S0009-2541(99)00086-8

1. Introduction

Although the isotopic composition of both organic and inorganic carbon has been studied extensively (e.g., Deines, 1980), the two typically have been studied in isolation. Secular trends in inorganic carbon, primarily as measured in carbonate minerals, have received the most attention (e.g., Scholle and Arthur, 1980; Shackleton, 1985), for it was recognized early on that the isotopic composition of the ocean could be reconstructed from the isotopic composition of well-preserved marine carbonates (fossils and cements) (Keith and Weber, 1964; Schidlowski et al., 1975). One then could use isotopic balance arguments to estimate changes in carbon cycling in the geologic past (Veizer and Hoefs, 1976; Garrels and Lerman, 1981; Holland, 1984; Holser, 1984; Kump and Garrels, 1986).

Recently, though, temporal trends in the carbon isotopic composition of organic matter have become established (see Hayes et al., this volume). Particularly intriguing has been the unusually ^{13}C-depleted organic matter in Cretaceous marine sediments, relative to the Neogene to Recent (Arthur et al., 1985; Dean et al., 1986); Hayes et al. (this volume) also have demonstrated that ^{13}C-depleted organic matter in marine sedimentary rocks is typical of the Phanerozoic as a whole. A variety of explanations has been explored, but the most promising interpretation continues to be that elevated aqueous CO_2 concentrations (equilibrated with a CO_2-enriched Cretaceous atmosphere) allowed for greater discrimination during algal photosynthesis, resulting in isotopically depleted organic material relative to organic matter in younger rocks. This observation led to the recognition that the isotopic difference between the burial fluxes of sedimentary organic matter (δ_{org}) and carbonate (δ_{carb}; i.e., $\Delta_B = \delta_{org} - \delta_{carb}$) could be used as a proxy for atmospheric pCO_2 in the geologic past (Dean et al., 1986; Freeman and Hayes, 1992; Popp et al., 1989; Rau et al., 1989; Jasper and Hayes, 1990; Hollander and McKenzie, 1991). However, Δ_B can differ from the primary photosynthetic isotope effect (ε_p) because of diagenetic overprints on either organic or carbonate carbon isotopic compositions (see Hayes et al., this volume). Moreover, recent investigations have revealed that the algal photosynthetic isotope effect is not only a function of environmental CO_2 concentrations, but of growth rates and temperature as well (Rau et al., 1992, 1997; Hinga et al., 1994; Bidigare et al., 1997). This clearly complicates the direct use of Δ_B as a pCO_2 proxy. However, if sufficient sampling is performed for a given time interval, temporal trends in global averages could still provide a measure of changes in atmospheric pCO_2 over Earth history. A number of recent studies have provided paired analyses of inorganic and organic carbon (Arthur et al., 1988; Lini et al., 1992; Magaritz et al., 1992; Jasper et al., 1994; Kump et al., 1995; Joachimski, 1997; Patzkowski et al., 1997). This analysis of both inorganic and organic carbon isotopic compositions on the same samples is essential, to avoid the persistent problem of correlation between carbonate- and shale- (organic-carbon-bearing) dominated sequences. As we will demonstrate below, the timing of the peaks and valleys of the two secular carbon isotope records may not coincide, even when subject to the same forcing. Thus, such carbon isotope curves cannot be used infallibly as a correlation tool.

We adopt the optimistic view that globally representative values will be obtained for the isotopic composition of both inorganic and organic carbon for the geologic past, and explore how these two might respond to a variety of geologically relevant forcings. We begin by presenting a simple box model for the carbon isotopic systematics of the ocean, and perturb it by increasing the organic-carbon burial rate above the presumed steady-state value. We then compare two simulations, one with fixed carbon isotopic discrimination by phytoplankton and another in which this factor is allowed to vary with CO_2 in a predictable way. Additional complexity is added to the model to examine possible isotopic consequences of increased volcanism and decreased rates of silicate weathering on land, both of which should tend to drive atmospheric pCO_2 to higher levels assuming constant burial rates of organic matter and carbonate. The effects of changing proportions of limestone and sedimentary organic matter weathering on oceanic isotopic composition also are explored, as are the consequences of an independent change in Δ_B (driven by the evolution of the C_4 photosynthetic pathway). These simulations are compared to iso-

topic records of carbonate and organic carbon, in an attempt to isolate the likely causes of isotopic excursions in the geologic past.

2. Model description

The mass-balance model for inorganic carbon and its stable isotopes in the ocean/atmosphere system is derived from Kump (1991) (Fig. 1). The amount of inorganic carbon in the ocean and atmosphere (M_o) changes on multimillennial time scales primarily as the result of imbalances between the inputs of carbon from weathering (F_w) and metamorphism/volcanism (F_{volc}), and the sediment burial outputs as organic matter ($F_{b,org}$) and carbonate minerals ($F_{b,carb}$):

$$\frac{dM_o}{dt} = F_w + F_{volc} - (F_{b,org} + F_{b,carb}) \quad (1)$$

The associated change in the carbon isotopic composition of the oceanic carbon reservoir, as reflected in the isotopic composition of carbonate sediments deposited from it, (δ_{carb}) can be represented as:

$$\frac{d}{dt}(M_o \delta_{carb}) = F_w \delta_w + F_{volc} \delta_{volc} - F_{b,carb} \delta_{carb} - F_{b,org}(\delta_{carb} + \Delta_B) \quad (2)$$

where δ_w is the average carbon isotopic composition of the riverine input (which reflects inputs from both carbonate–mineral and ancient organic carbon weathering), δ_{volc} is the isotopic composition of the volcanic and metamorphic flux, and Δ_B represents the isotopic difference between the organic matter and carbonate deposited from the ocean, expressed here as a negative number. (Actually δ_{carb} is enriched by 1–2‰ relative to the isotopic composition of dissolved inorganic carbon in the ocean.)

Presuming, as others have in the past (e.g., Garrels and Lerman, 1984; Kump and Garrels, 1986;

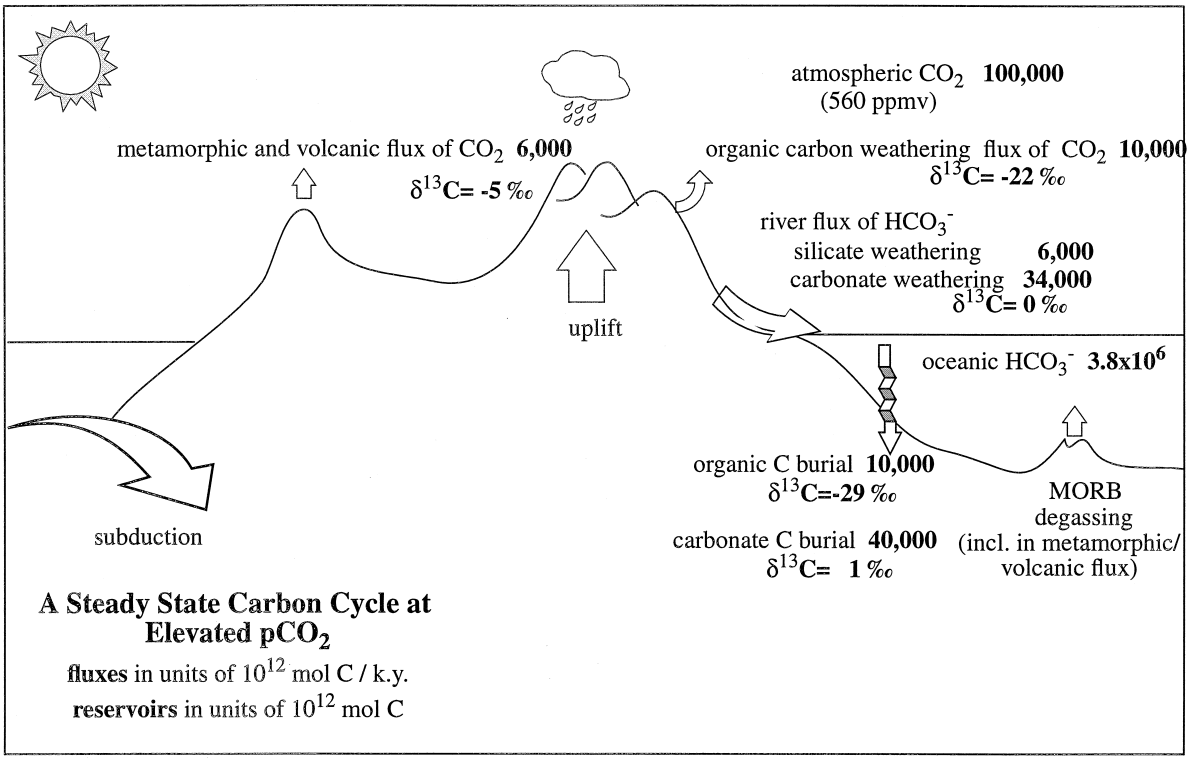

Fig. 1. The long-term carbon cycle, showing fluxes and isotopic compositions. The values shown establish a steady state that is used as the basis for the sensitivity analyses of subsequent diagrams. Values are presumed to be reasonably representative of the Phanerozoic average state.

Holser et al., 1988), that both δ_{volc} and δ_w approximate the 'mantle' value, we can lump the volcanic flux into the weathering flux and call it F'_w. Then, using the product rule of calculus and substituting Eq. (1) into Eq. (2) we arrive at the simplified time-dependent equation for δ_{carb}:

$$\frac{d\delta_{carb}}{dt} = \frac{F'_w(\delta'_w - \delta_{carb}) - F_{b,org}\Delta_B}{M_o} \quad (3)$$

Note that the only steady-state assumptions made so far are that the ocean is well-mixed and the exchange of carbon between the oceans and atmosphere is in steady state; we have not assumed that the mass or isotopic composition of the ocean as a whole are in steady state. Nevertheless, the resulting equation is quite simple. It states that the isotopic composition of the ocean may change with time due to imbalances in isotopic fluxes because the isotopic compositions of the riverine input and organic output differ from δ_{carb}. The amount of carbon in the ocean only affects the magnitude of the rate of change; this term drops out at steady state.

2.1. Steady state

At steady state (a general assumption valid for timescales long with respect to the residence time of carbon in the ocean/atmosphere, which today is about 10^5 years), the weathering input is balanced by the sum of organic carbon and carbonate burial (Eq. (1)). Moreover, the derivative expressed in Eq. (3) is zero. Therefore, the organic fraction (f_{org}) of the total carbon burial flux can be found by setting Eq. (3) to zero and dividing through by F'_w ($= F_{b,org} + F_{b,carb}$). Doing so yields the following:

$$f_{org} = \frac{(\delta'_w - \delta_{carb})}{\Delta_B} \quad (4)$$

This is the canonical expression most often used to interpret carbon-isotope excursions as reflecting changes in organic carbon burial rates (the 'lever' rule of Holland, 1984). It clearly indicates that to do so, however, one must either independently determine δ'_w and Δ_B or assume them constant. One must also presume some knowledge of the total carbon throughput rate (i.e., F'_w). These factors likely have varied considerably over geologic time, so we will explore the model's response to them. δ_{carb} can, of course, be determined reasonably well by analysis of well-preserved marine carbonate minerals. Δ_B is determined as the difference between δ_{org} and δ_{carb}. δ'_w is more difficult to determine directly and is most readily estimated using estimates of the relative volumes of rocks of different compositions being weathered using paleogeologic maps (e.g., Bluth and Kump, 1991; Gibbs and Kump, 1994).

2.2. Equilibration of the ocean / atmosphere system with $CaCO_3$

To be able to explore the consequences of the possible dependence of Δ_B on atmospheric pCO_2, we need a relationship that relates atmospheric pCO_2 to M_o. The simplest relationship presumes that the ocean as a whole remains essentially saturated with respect to $CaCO_3$ and equilibrated with atmospheric CO_2 through geologic time (e.g., Broecker and Peng, 1982, 1987):

$$2HCO_3^-(\text{ocean}) + Ca^{2+}(\text{ocean}) = CaCO_3(\text{sed}) + H_2O + CO_2(\text{atm}) \quad (5)$$

and

$$K = \frac{M_{Ca} M^2_{HCO_3^-}}{pCO_2}, \quad (6)$$

an assumption that may not be valid for intervals of dramatic environmental change (e.g., Grotzinger and Knoll, 1995). The use of Eq. (6) in our simulations can be simplified by holding M_{Ca} constant, adopting the simplification that M_o is essentially $M_{HCO_3^-}$ (the oceanic bicarbonate content) at typical oceanic pH values, and scaling M_o and atmospheric pCO_2 contents to today's values. Then paleoatmospheric pCO_2 can be determined from M_o according to the following simple relationship:

$$pCO_2(t) = \left(\frac{M_o(t)}{M_o(0)}\right)^2 pCO_2(0) \quad (7)$$

This relationship states that atmospheric pCO_2 changes in proportion to the square of changes in the total inorganic carbon content of the ocean, under the conditions specified. Among the assumptions implied is that there are no large changes in mean

oceanic temperature on the time scales considered. The assumption that M_{Ca} is constant on the timescale of the perturbation studied here ($\sim 10^5$ years) is probably valid because of the relatively long residence time of Ca in the ocean (~ 1 m.y.; Holland, 1984).

2.3. Photosynthetic isotope effect and atmospheric pCO_2

Many attempts have been made to calibrate the photosynthetic isotope effect (ε_p) for marine algae against CO_2 concentration, and each attempt has yielded a somewhat different calibration (e.g., Freeman and Hayes, 1992; Hinga et al., 1994; Maslin et al., 1996; Bidigare et al., 1997). In the modern ocean, ε_p varies by nearly 8‰ as a function primarily of variations in surface–water pCO_2 and growth rate, both of which exhibit latitudinal trends (e.g., Rau et al., 1997). Some calibrations in the literature are based on these trends, whereas others are based on laboratory experiments. We chose to use the Bidigare et al. (1997) data set for haptophyte algae, which relates ε_p to $[CO_2(aq)]$ and requires knowledge of dissolved phosphate concentrations in surface waters. Pagani et al. (in review) fit the data using a geometric mean assumption and developed the following equation, assuming a maximum enzymatic isotope effect of 25‰ (here ε_p is positive by convention):

$$25 - \varepsilon_p = \frac{(159.5[PO_4]) + 38.39}{[CO_2(aq)]} \quad (8)$$

At 25°C (a reasonable average low-latitude temperature),

$$\varepsilon_p = -(\Delta_B + 8) \quad (9)$$

as the result of equilibrium fractionation between inorganic carbon species. We can then rearrange Eq. (8), substituting atmospheric pCO_2 for $[CO_2(aq)]$, assuming equilibration according to Henry's Law at 25°C, and using Eq. (9) for ε_p, to obtain an expression relating Δ_B to pCO_2:

$$\Delta_B = \left(\frac{(159.5[PO_4]) + 38.39}{0.034\, pCO_2} \right) - 33. \quad (10)$$

This relationship is shown in Fig. 2, with $[PO_4] = 0.25$ μmol/kg, a typical oligotrophic surface-ocean

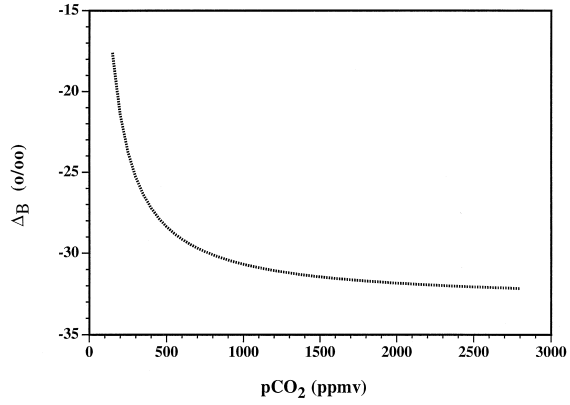

Fig. 2. A generic response curve for the dependence of the isotopic difference between carbonate and organic carbon (Δ_B) on ambient pCO_2. The relationship is not inconsistent with the range of calibrations presented in the literature, and is based on the work of Bidigare et al. (1997). It presumes equilibration between the surface ocean and atmosphere, and neglects the effects of growth-rate and temperature dependence, and diagenesis, on Δ_B.

value. There is some suggestion that the asymptote (~ -33‰) could be at higher pCO_2 than assumed here. For example, the Hinga et al. (1994) data suggest saturation at around 1500 ppmv, whereas the Bidigare et al. data suggest a value closer to 1000 ppmv. If so, this would make the model-derived δ_{org} more sensitive at higher pCO_2.

Also note that we have ignored possible growth-rate effects on δ_{org} (e.g., Laws et al., 1995; Bidigare et al., 1997; Hayes et al., this volume) because we assume that most of the geologic data we will compare our model results to come from oligotrophic regions. We also ignore the possibility that the ε_p of terrestrial plants may not respond as sensitively to changes in atmospheric pCO_2 as marine algae (e.g., Popp et al., 1989). The contribution of terrestrial organic matter to global organic carbon sedimentation through time is unknown, but likely to be significant since the Late Devonian (e.g., Kump, 1993). For simplicity, however, we treat the isotopic consequences of changes in organic carbon burial as if the material was entirely marine in origin.

2.4. Carbon inputs to the ocean / atmosphere system

The isotopic composition of the combined weathering flux, δ_w, is primarily set by the relative proportions of carbonate–mineral and ancient organic car-

bon weathering. For most simulations, this value is set at −5‰, although in one simulation we force the model with a reduction in the weathering contribution from organic carbon, which drives the riverine value toward heavier values. We thus need to distinguish between the organic ($F_{w,org}$), carbonate ($F_{w,carb}$), and silicate ($F_{w,sil}$) weathering inputs. F_w in the above equations is actually:

$$F_w = F_{w,carb} + F_{w,org}; \quad (11)$$

$F_{w,sil}$ does not appear in this equation because it does not add or subtract carbon from the ocean/atmosphere system, it simply converts one form of inorganic carbon (atmospheric CO_2) into another (oceanic HCO_3^-). Recall that we are only considering carbon fluxes, not cation fluxes.

We can simplify this expression somewhat and, in the process, Eq. (1) as well by recognizing that the carbonate ion concentration, and thus the carbonate mineral burial rate ($F_{b,carb}$) responds an order of magnitude faster than M_o to flux imbalances at today's M_o and oceanic pH (Broecker and Peng, 1987; Gibbs and Kump, 1994). Thus, we can assume that the inputs and outputs of alkalinity are in quasi-steady state, and thus that:

$$F_{w,carb} + F_{w,sil} = F_{b,carb}. \quad (12)$$

Then we can rewrite Eq. (1) as

$$\frac{dM_o}{dt} = F_{w,org} + F_{volc} - F_{b,org} - F_{w,sil} \quad (13)$$

Note here that $F_{w,sil}$ appears as a sink rather than a source for carbon in the ocean/atmosphere system, because we are assuming that the ocean responds instantaneously to silicate weathering production of alkalinity by depositing $CaCO_3$. Eq. (13) is a restatement of the long-term carbon balance, which states that sources of CO_2 to the ocean/atmosphere system are balanced (the derivative is zero) on long time scales by the sinks for CO_2 associated with organic carbon burial and silicate weathering.

3. Model results

We now have a pair of differential equations (Eqs. (3) and (13)) that can be solved numerically given the other relationships described above, and used to investigate the possible causes of isotopic excursions in the geologic past. In these simulations we first establish a baseline steady state, then apply perturbations for 500 ky, and finally return the forcing to its original value, allowing the system to adjust to a new steady state (which may be different from the original). We have chosen to establish this steady state at an atmospheric pCO_2 of 560 ppm (Fig. 1), twice the pre-industrial value, because we assume that most of geologic time was marked by somewhat higher pCO_2 (Berner, 1994) and resulting overall warmer climates (Fischer, 1982). The resultant Δ_B (from Fig. 2) is −29‰ (slightly depleted compared to the canonical value of −25‰), a number more consistent with δ_{org} values from much of the Phanerozoic (Dean et al., 1986; Hayes et al., this volume). Isotopic balance then demands a steady-state $\delta_{carb} = 0.78‰$ (slightly elevated relative to the canonical value of 0‰).

3.1. Perturbation 1: increased organic carbon burial

The most common interpretation of positive excursions in δ_{carb} (as recorded in marine limestones) is that they reflect increases in global organic-carbon burial rates either by increased marine phytoplankton productivity or increased preservation under anoxic waters. Negative excursions have been interpreted to represent the opposite. Perhaps the most studied of the negative excursions occurred at the Cretaceous–Tertiary (K–T) boundary (Zachos et al., 1989). Kump (1991) demonstrated with a two-box model of the ocean that excursions in surface–water carbon isotopic composition like that at the K–T boundary, which last more than a few tens of thousands of years, reflect changes in the overall isotopic balance of the ocean, and must be interpreted in terms of changes in either the input or output of carbon from the ocean. In interpreting organic carbon burial rates from the isotopic record, one must also realize that what is actually being recorded is the organic carbon burial fraction (f_{org}). To interpret carbon isotopic excursions in terms of actual flux changes, one must have independent evidence concerning the total carbon throughput (in both inorganic and organic forms) of the ocean. Even in interpreting the carbon isotopic record as changes in f_{org}, one must either specify changes in Δ_B and δ_w or assume them constant. Eq.

(4) shows that with constant Δ_B and δ_w, changes in organic carbon burial rate ($F_{b,org}$) are linearly recorded by δ_{carb}. For example, by specifying that $\Delta_B = -29‰$ and $\delta_w = -5‰$, we would interpret an isotopic shift in δ_{carb} from 0.8‰ to 3.6‰ as representing a 50% increase in f_{org} from 0.2 to 0.3, and, assuming the total carbon burial flux remains constant, a 50% increase in the organic carbon burial rate. This, of course, is independent of the *cause* of increased relative organic carbon burial (e.g., either enhanced productivity or preservation). Sometimes higher marine productivity is inferred, but such inferences rest on a rather tenuous link between productivity and burial involving the vagaries of remineralization in the water column and preservation in the sediment. Many organic-carbon burial events may represent a combination of causes inasmuch as high productivity and oxygen deficiency are commonly linked (see review by Arthur and Sageman, 1994).

The time-dependent equation (Eq. (3)) can be solved to investigate the response of the system to persistent forcings or instantaneous changes. To simulate an increase in organic carbon burial ($F_{b,org}$), we either 1) instantaneously increase the riverine supply of phosphate to the ocean, 2) increase the fraction of phosphate-driven new production that survives decomposition to be buried ($f_{preserv}$), or 3) increase the deep-water turnover rate, which increases the supply of phosphate to the euphotic zone, in all cases by 50%. In all cases we also assume that phosphate availability limits productivity (Broecker and Peng, 1982), and adopt an initial phosphate residence time of 10^5 years. For the runs with fixed $f_{preserv}$, we choose a preservation fraction of 0.01, a canonical value from Broecker and Peng (1982).

3.1.1. Increased riverine phosphate delivery

In this simulation, we begin with a 'standard' case, one which embodies the common assumptions of simple models of $\delta^{13}C$ excursions. Applying a 50% increase in riverine phosphate input to the model, and assuming fixed Δ_B, results in the following responses: (1) The phosphate concentration increases asymptotically to 150% of its original concentration during the period of perturbation, then returns to its original concentration with a response (e-folding) time of around 10^5 years. As a result, the organic carbon burial rate increases to a value 150% of its original rate and then falls along the same trajectory as dissolved phosphate; and (2) atmospheric pCO_2 is reduced from the original value (560 ppm) to $\sim$155 ppm (Fig. 3a). Atmospheric pCO_2 does not achieve steady state during the perturbation, despite its potentially more rapid response time, because there is no feedback mechanism for stabilizing atmospheric pCO_2 in the model (i.e., no mechanism of compensating for the increased output of organic carbon from the atmosphere/ocean system by either increasing a source or decreasing another sink), and so atmospheric pCO_2 continues to fall until the perturbation is removed. We address this shortcoming later.

The isotopic response is as expected from our consideration of steady states above: δ_{carb} increases to +3.6‰, and then returns to the steady-state value of 0.8‰ after the perturbation is removed (Fig. 3b). Because Δ_B is fixed, the organic carbon isotopic response tracks the inorganic response, with a con-

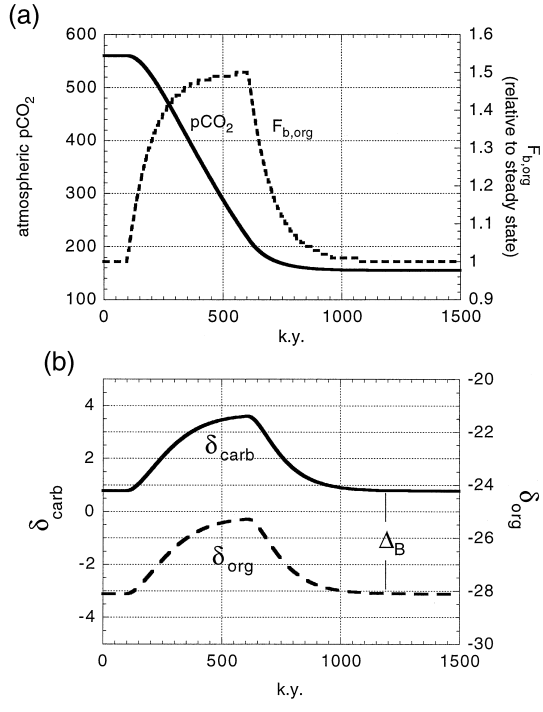

Fig. 3. The response of (a) the global organic carbon burial rate and atmospheric pCO_2 and (b) the inorganic- and organic-carbon isotopic composition of marine sediments to a 50% increase in the rate of phosphate delivery rate to the ocean that persists for 500 ky, assuming constant Δ_B.

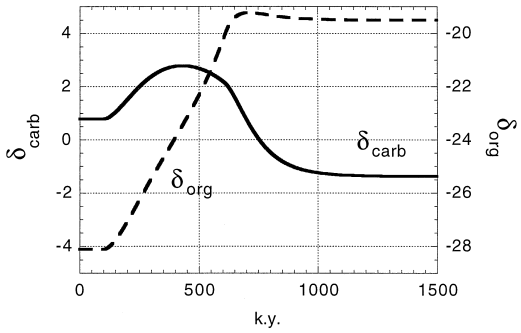

Fig. 4. The response of the inorganic- and organic-carbon isotopic composition to a 50% increase in the riverine phosphate delivery rate (Fig. 3a) applied for 500 ky, assuming variable Δ_B according to Fig. 2.

stant offset equal to Δ_B. Both values eventually experience the 2.8‰ increase expected from steady-state considerations described above.

The isotopic response to a doubling of the organic carbon burial rate is somewhat different if we allow Δ_B to be a function of atmospheric pCO_2 (i.e., applying Fig. 2). In this case, δ_{carb} only reaches a peak value of 2.8‰ as compared to 3.6‰ in the previous case (Fig. 4). δ_{carb} then begins to decline before the perturbation in organic carbon burial is removed, whereas in the previous case, and implicit in most interpretations of δ_{carb} records, the reversal in trend toward declining values occurs simultaneously with the end of the high burial rate episode. This reversal prior to a decrease in $F_{b,org}$ (Fig. 3a) is the result of the drawdown in atmospheric pCO_2, which causes a reduction in Δ_B. The positive excursion in δ_{org} $(= \delta_{carb} + \Delta_B)$ is thus larger than that of δ_{carb}, and the peak value occurs later. Once the perturbation is removed, the system evolves back to steady state, reaching the original fluxes but characterized by a more ^{13}C-depleted δ_{carb} and ^{13}C-enriched δ_{org} that reflects the reduced Δ_B resulting from lowered atmospheric pCO_2. Note that in this model the overall shift in δ_{carb} resulting from an organic-carbon burial event is a *negative* excursion because of the adjustment in Δ_B and the lack of any stipulated feedback to restore atmospheric pCO_2 to its pre-perturbation level.

Despite their appealing simplicity, the previous two simulations are unrealistic because they disconnect riverine phosphate input from the riverine carbon input. One consequence of neglecting this connection is that the oceanic/atmospheric carbon reservoir is drawn down more rapidly (Fig. 3a) than it would be if we had allowed riverine carbon inputs (especially those from carbonate and organic carbon weathering, represented by F_w) to track phosphate input. Moreover, the extra input of isotopically depleted carbon from greater riverine flux is ignored. To address this deficiency, we can impose the same 50% increase on $F_{w,sil}$ and F_w as we do on the phosphate delivery rate. The response in the model becomes more complicated than in previous cases. Atmospheric pCO_2 actually rises slightly at first, the result of increased F_w (Fig. 5a). Then it falls, but not to the low levels of previous simulations (Fig. 3a) despite the fact that the change in $F_{b,org}$ is identical in all cases examined so far. The new steady-state atmospheric pCO_2 is 290 ppm, compared to

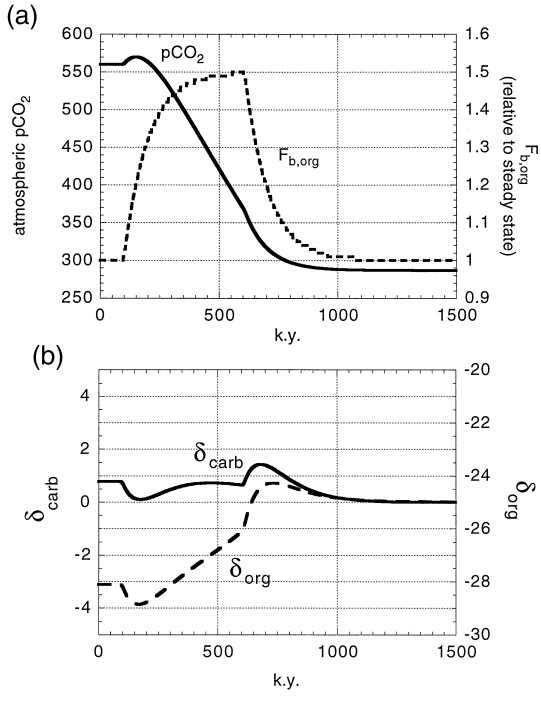

Fig. 5. The response of (a) the global organic carbon burial rate and atmospheric pCO_2 and (b) the inorganic- and organic-carbon isotopic composition of the marine sediments to a 50% increase in the rate of riverine phosphate and inorganic carbon delivery rate to the ocean that persists for 500 ky. This case differs from Fig. 3 in that the other riverine fluxes of inorganic carbon from weathering are also assumed to increase by 50%.

155 ppm in the previous simulation, because of the added carbon input from organic carbon weathering.

In response to the instantaneous increase in the delivery of depleted carbon associated with F_w, δ_{carb} falls to near 0‰ in the first 10^5 years of the perturbation (Fig. 5b). It then rises in two steps: one in response to enhanced organic-carbon burial, muted, as in Fig. 4, by the instantaneous reduction in Δ_B, and another rise once the perturbation is removed, in response to the reduction in riverine delivery of depleted carbon to the ocean/atmosphere system. The peak value in δ_{carb}, 1.4‰, represents a small excursion in comparison to earlier scenarios, and it occurs after the 500 ky interval of enhanced organic carbon burial. In this simulation δ_{org} more closely tracks δ_{carb}, with a large amplitude of change relative to δ_{carb} but a smaller amplitude than in the previous simulation (4‰ compared to 9‰), because the reduction in atmospheric pCO_2 was smaller.

Under extremely high atmospheric pCO_2, Δ_B is maximized (Fig. 2), and further increases or small decreases in pCO_2 have little effect on Δ_B. To demonstrate this effect, we apply the same 50% increase in riverine phosphate delivery to a model pre-equilibrated with an atmosphere at $10\times$ the present atmospheric level (2800 ppm). In this simulation δ_{carb} and δ_{org} respond in parallel to the forcing, and independent of atmospheric pCO_2 (Fig. 6). In reality, the CO_2 concentration at which the photosynthetic isotope effect is maximized apparently varies from one phytoplankton group to another, and is likely to have evolved in response to changes in ambient CO_2 concentrations. Also, the contributions to marine sediments of terrestrial organic matter, whose isotopic composition may be insensitive to atmospheric pCO_2, are poorly known. Thus, a precise interpretation of the isotopic record in terms of atmospheric pCO_2 is difficult to justify, although trends can certainly be inferred.

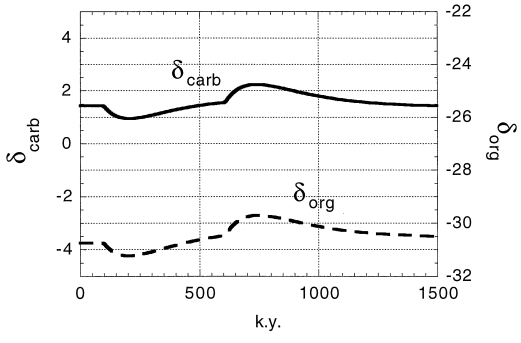

Fig. 6. The response of the inorganic- and organic-carbon isotopic composition to a 50% increase in riverine phosphate and inorganic carbon delivery rate, applied for 500 ky to a system initially equilibrated at 2800 ppmv pCO_2, assuming variable Δ_B (Fig. 2).

This exercise highlights the resistance of the natural system to change, both in terms of reservoir size and isotopic composition. Increased organic-carbon burial in a phosphate-limited world requires increased weathering and riverine delivery of phosphate, and this is accompanied by isotopically depleted inorganic carbon that damps the reservoir change and the excursion in its isotopic composition.

3.1.2. Increased thermohaline circulation or organic carbon preservation

One can envision other ways in which organic-carbon burial may increase, and cause a positive δ_{carb} excursion. For example, reduced remineralization efficiency in the water-column and sediment (i.e., greater preservation potential, $f_{preserv}$) could lead to a $F_{b,org}$ increase, perhaps the result of decreased thermohaline circulation (e.g., Bralower and Thierstein, 1984). Another invokes *increased* thermohaline circulation, which provides a greater upwelling nutrient flux to the surface (e.g., Late Ordovician: Brenchley et al., 1995). Applying a 50% increase to either preservation or circulation leads to the same response: the organic carbon burial rate ($F_{b,org}$) increases by 50% instantaneously, but then returns rapidly to the original value as the oceanic phosphate reservoir decreases to $2/3$ of its original value (Fig. 7a), thus compensating for the $3/2$ increase in circulation rate or preservation fraction (assuming constant river influx). When either perturbation is relaxed, the oceanic phosphate concentration returns to its original value with a 10^5-year response time (cf. Broecker and Peng, 1982). However, organic-carbon burial rates ($F_{b,org}$) initially experience a further, but temporary fall during this transition. This is because the turnover rate or the preservation factor has returned to its initial, lower value, and the phosphate reservoir is still depleted. During this perturbation, atmospheric pCO_2 falls only by about 70 ppm (Fig. 7a), and reaches a near steady state by the end of the perturbation. This steady state is achieved because

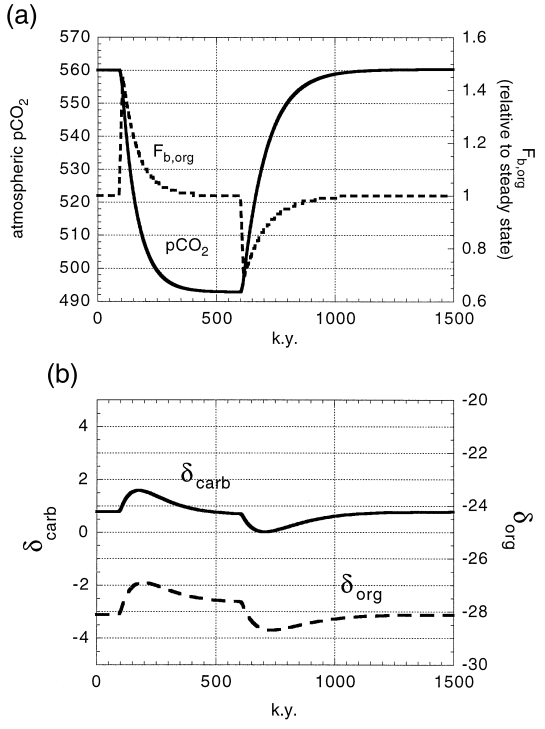

Fig. 7. The response of (a) the global organic carbon burial rate and atmospheric pCO_2 and (b) the inorganic- and organic-carbon isotopic composition of marine sediments to a 50% increase in the thermohaline circulation rate (or organic carbon preservation percentage) of the ocean that persists for 500 ky.

$F_{b,org}$ returns to its original value 10^5 years after the perturbation is applied and the sources and sinks for carbon come into balance. When the perturbation is removed, atmospheric pCO_2 very quickly returns to its initial value, because productivity and organic carbon burial are temporarily reduced below the steady-state values.

The immediate carbon isotopic response to increased turnover or preservation (and thus increased $F_{b,org}$) is one of enrichment in ^{13}C, slightly magnified in δ_{org} relative to δ_{carb} because of the reduction in atmospheric pCO_2 (Fig. 7b). The reduction in $F_{b,org}$ associated with the end of the perturbation causes a transient negative isotopic excursion in both δ_{carb} and δ_{org}. Ultimately there is no vestige of the 500 ky excursion in either atmospheric pCO_2 or the isotopic composition of either the carbonates or organic carbon: the system has returned completely to its original state.

3.1.3. Model-data comparison I: Cenomanian–Turonian isotopic excursion

The Cretaceous Cenomanian–Turonian (C/T) boundary interval is a well-studied global event associated with a positive carbon isotope excursion (Arthur et al., 1988) lasting 1 m.y. The positive excursion has been interpreted as reflecting an increase in organic carbon burial rate and drawdown in atmospheric pCO_2 (Arthur et al., 1988). A high-resolution record of both inorganic and organic carbon isotopes for this event from the US Western Interior Seaway (Hayes et al., 1989; Pratt et al., 1993) is reproduced in Fig. 8. These data indicate that in the mid- to late-Cenomanian, prior to the excursion, Δ_B was approximately $-28‰$. During the event, δ_{org} increased by 4‰, while δ_{carb} only increased about 2‰, indicating that Δ_B fell (in absolute magnitude) to $-26‰$. This reduction in Δ_B has been generally attributed to a decline in atmospheric pCO_2 (Arthur et al., 1988), although Hayes et al. (1989) emphasize the importance of considering alternative hypotheses, e.g., possible changes in species composition of primary producers and/or differential processing of organic matter in the water column by heterotrophs.

None of our simulations produce a pattern that matches the C/T record satisfactorily. The initial simulation (Fig. 3b) produced parallel isotope excursions in δ_{carb} and δ_{org}, but had fixed Δ_B and thus did not generate a larger excursion in δ_{org} compared to δ_{carb}. Allowing Δ_B to respond to the reduction in

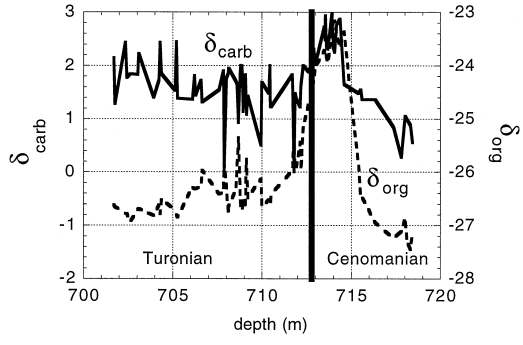

Fig. 8. Carbon isotopic excursion in whole-rock carbonate (δ_{carb}) and total organic carbon (δ_{org}) at the Cretaceous Cenomanian/Turonian boundary (Hayes et al., 1989). The C/T boundary occurs at ~713 m in this section. Time runs forward to the left, and the total amount of time represented is on the order of 1 million years.

atmospheric pCO_2 creates a larger excursion in δ_{org} (Fig. 4), but 1) the peak in δ_{org} occurs after the δ_{carb} peak, and 2) δ_{org} remains 'permanently' ^{13}C-enriched after the perturbation, because atmospheric pCO_2 is low. Increased thermohaline circulation, a mechanism invoked by Arthur et al. (1987) to explain the C/T event, or increased $f_{preserv}$, also create parallel excursions under the conditions we imposed (Fig. 7b). However, not only are the excursions small, but the atmospheric pCO_2 drawdown and thus the change in Δ_B is minimal. Linking F_w and F_{wsil} to phosphate input (Fig. 5b) generates an isotopic response that more closely resembles the data, but once again, pCO_2 remains low, and δ_{org} high.

Perhaps our neglect of restorative CO_2 feedbacks (e.g., the carbonate–silicate cycle; Berner et al., 1983) is responsible for our inability to simulate the C/T event. We test this idea by applying a simple, linear dependence of $F_{w,sil}$ on atmospheric pCO_2:

$$F_{w,sil} = F^0_{w,sil}\frac{pCO_2(t)}{pCO_2(0)}, \quad (14)$$

under the constraints of the model that generated the curves in Fig. 5a and 5b (instantaneous 50% increase in all weathering fluxes, variable Δ_B), where $F^0_{w,sil}$ is the steady-state silicate weathering rate (Fig. 1). Now, with the CO_2-weathering feedback, atmospheric pCO_2 rebounds after the perturbation is removed (Fig. 9a). As a result, δ_{org} and δ_{carb} both return to their initial values after an interval of ^{13}C enrichment accompanying the cessation of elevated riverine delivery (Fig. 9b).

In many of these simulations, the isotopic changes are abrupt, a consequence of the instantaneous appli-

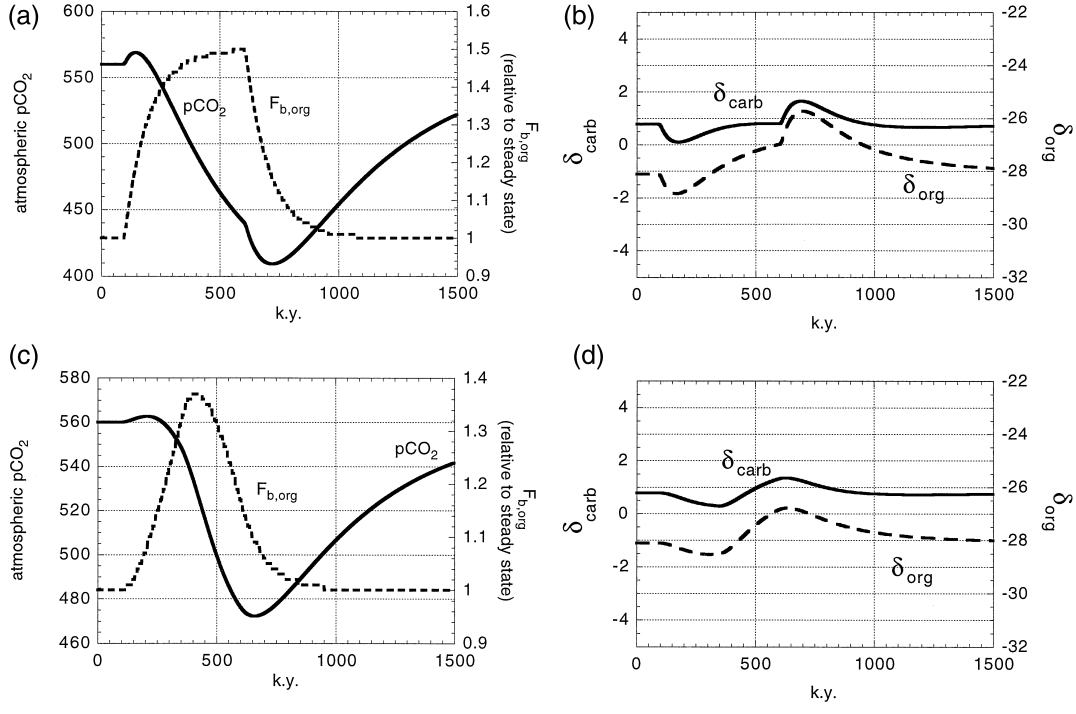

Fig. 9. The response of (a) the global organic carbon burial rate and atmospheric pCO_2 and (b) the inorganic- and organic-carbon isotopic composition of marine sediments to a 50% increase in the rate of riverine phosphate and inorganic carbon delivery rate to the ocean that persists for 500 ky. This case differs from that shown in Fig. 5 because the silicate weathering rate is assumed to be linearly dependent on atmospheric pCO_2. A more gradual change in the rate of riverine phosphate and inorganic carbon delivery rate to the ocean, in which the riverine flux increases gradually over the first 250 ky to 50% above the steady state, and then declines back to the steady state value over the next 250 ky, leads to a more gradual response in (c) the global organic carbon burial rate and atmospheric pCO_2 and (d) the inorganic- and organic-carbon isotopic composition of marine sediments.

cation and remove of the perturbations. To show that the overall responses (e.g., the initial negative δ_{carb} excursions) are not an artifact of instantaneously increasing the riverine P supply, we apply the increase gradually (over the first 250 ky of the perturbation) and then withdraw it symmetrically over the second half of the perturbation (Fig. 9c). The pCO_2 (Fig. 9c) and isotopic (Fig. 9d) responses are qualitatively similar to those before (Fig. 9a and 9b), although the magnitudes of the excursions are smaller. Either set of isotopic predictions matches the character of the isotopic signature of the C/T record (Fig. 8).

The notion that riverine inputs increased dramatically in the Late Cenomanian and suddenly diminished in the earliest Turonian is new, and not precluded by available data. However, our analysis also does not preclude increased thermohaline circulation as a cause of the event. One could envision a more complicated history of overturn and oceanic phosphate buildup that could produce the observed isotopic response, but recall that our goal in this study is to show characteristic responses of simple models to allow differentiation of process-response scenarios for the geologic record.

3.1.4. Model-data comparison II: Late Middle Ordovician isotopic excursion

In contrast to the C/T event, the early Cretaceous (Valanginian) event of Lini et al. (1992) and the Late Middle Ordovician isotopic excursion reported by Patzkowski et al. (1997) are characterized by δ_{org} peaks that appear to lag major peaks in δ_{carb}. In the Ordovician case (Fig. 10), a parallel rise in δ_{carb} and δ_{org} in micrites is followed hundreds of thousands of years later by an abrupt increase in δ_{org}, coincident with a subtle reversal (fall of $\sim 0.5‰$) in δ_{carb}. Unfortunately, this record from central Pennsylvania does not extend to the end of the excursion, but comparison with the excursion in Iowa (Ludvigson et al., 1996) suggests that δ_{carb} continued to fall another 0.5‰. Based on the modeling described so far, we would interpret this record as an organic carbon burial event that began at highly elevated atmospheric pCO_2, and thus began with parallel excursions in both δ_{carb} and δ_{org}. As the event proceeded, high rates of organic carbon burial caused pCO_2 to fall into the range of sensitivity for Δ_B,

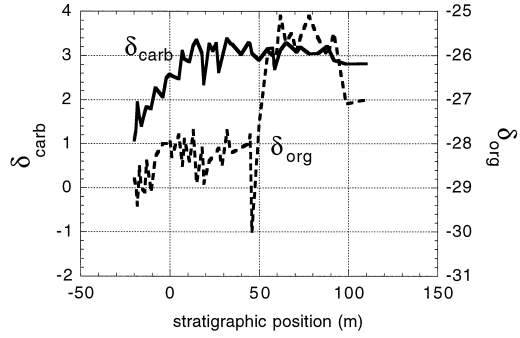

Fig. 10. The Late Middle Ordovician isotopic excursion reported by Patzkowski et al. (1997). Time is forward to the right along the abscissa; the amount of time represented is ≤ 1 m.y.

causing a marked increase in δ_{org} that should be mirrored by a slight decrease in δ_{carb} (the data are ambiguous in this regard).

3.1.5. Perturbation 2: increased volcanic CO_2 emanation

Intuition suggests that a geologically sudden increase in volcanism sufficient to perturb atmospheric pCO_2 levels should drive down the carbon isotopic value of the inorganic carbon in the ocean–atmosphere system (δ_{carb}). The effect would be transitory, though, because the isotopic composition of volcanic CO_2 is comparable to that of the riverine input; a change in volcanic input rate will not in and of itself drive a steady-state shift of δ_{carb}. Even during the transient phase the isotopic response might be less than expected, because Δ_B should increase in magnitude as atmospheric pCO_2 rises, and this should tend to counter the tendency toward reduced δ_{carb} because of isotope balance considerations. We can test these ideas quantitatively by applying an instantaneous 50% increase in volcanic CO_2 delivery, and let it persist for the standard 500 ky before relaxing the perturbation (Fig. 11a).

Upon initial application of the perturbation to the model with variable Δ_B, δ_{carb} declines as atmospheric pCO_2 climbs (Fig. 11a) and Δ_B increases in absolute magnitude (Fig. 11b). This trend in δ_{carb} is reversed within 200 ky as the burial of anomalously depleted organic matter overcompensates for additional input of depleted volcanic CO_2. As the perturbation is removed, δ_{carb} returns to steady state, but at a slightly more enriched value that compensates for

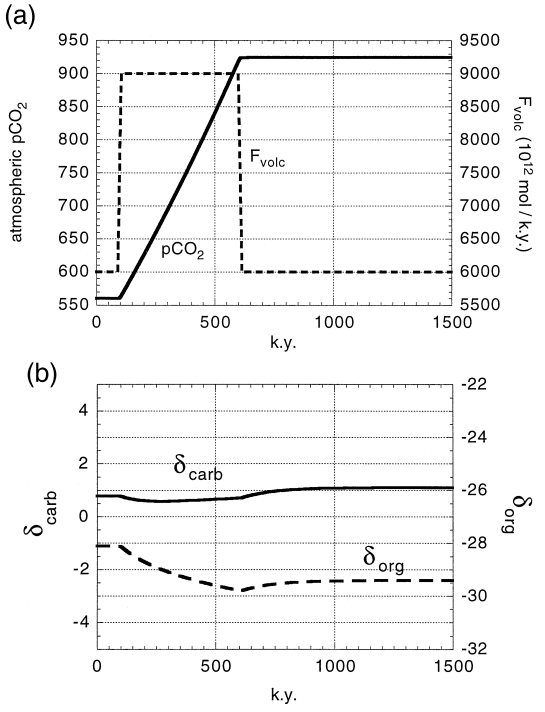

Fig. 11. The response of (a) atmospheric pCO_2 and (b) the inorganic- and organic-carbon isotopic composition of marine sediments to a 50% increase in the volcanic carbon input rate that persists for 500 ky.

the fact that organic carbon is now isotopically depleted in ^{13}C. This may seem counterintuitive: the ocean/atmosphere system has experienced a period of excess volcanic input of isotopically depleted carbon, and has become isotopically enriched. Any vestige of the input of volcanic carbon in the ocean/atmosphere inorganic carbon reservoir is removed within 200 ky. The isotopic composition of organic matter is depleted, and the overall shift in δ_{org} is considerably larger ($\sim -2‰$) than the shift in δ_{carb}. Thus, a large negative excursion in δ_{org}, unaccompanied by a large response in δ_{carb}, could be interpreted as a volcanically induced increase in atmospheric pCO_2.

3.1.6. Perturbation 3: decreased silicate weathering

Variations in the rate of silicate-mineral weathering over geologic time have likely resulted from changes in the area of exposure (Bluth and Kump, 1991) and relief (Stallard and Edmond, 1983; Raymo and Ruddiman, 1992; Kump and Arthur, 1997) of silicate-bearing rocks. These changes affect atmospheric pCO_2, and, through equilibration with the ocean (Eq. (5)), the total carbon of the ocean (e.g., Berner et al., 1983). The variations in themselves do not drive carbon isotopic response in the oceans because no rock-derived carbon is provided. However, the dependence of Δ_B on pCO_2 could generate an isotopic response.

The response of the model to a 50% reduction in the rate of silicate weathering is an increase in atmospheric pCO_2 (Fig. 12a) identical to that of a 50% increase in the volcanic input rate (the flux imbalance in both cases is 3000×10^{12} mol/ky). The isotopic excursions are similar, and identical at steady state (Fig. 12b). However, there is no transient depletion of δ_{carb} as seen when volcanism was doubled. Rather, δ_{carb} immediately increases as δ_{org} decreases in response to the increase in Δ_B with atmospheric pCO_2. The total carbonate isotopic excursion is small, only $\sim 0.4‰$, driven by the small proportional increase in the absolute value of Δ_B.

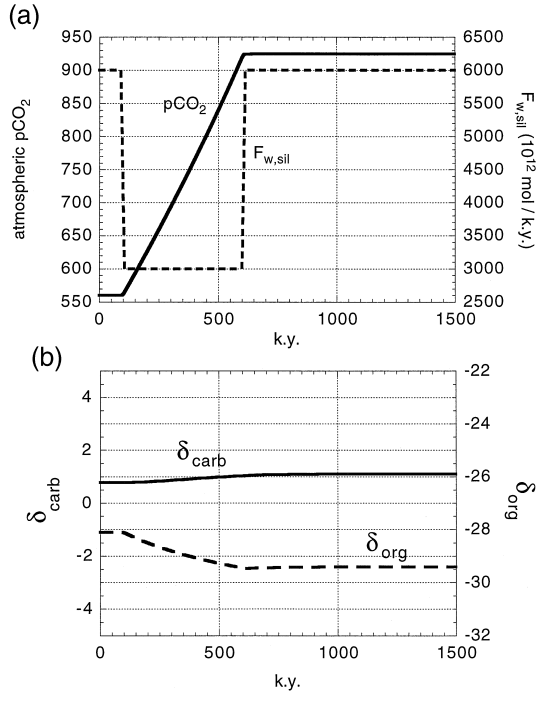

Fig. 12. The response of (a) atmospheric pCO_2 and (b) the inorganic- and organic-carbon isotopic composition of marine sediments to a 50% reduction in silicate weathering applied for 500 ky.

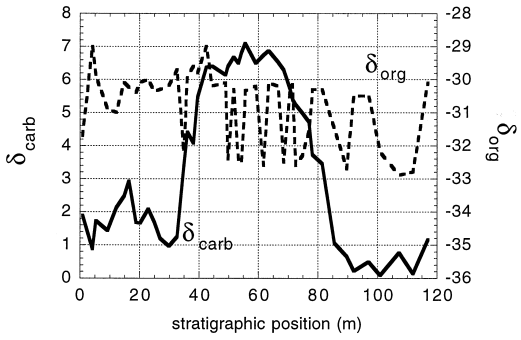

Fig. 13. Inorganic and organic carbon isotopic record of the latest Ordovician (Hirnantian) of the Copenhagen Canyon section, Nevada (Kump et al., in press). Time is forward to the right; the total duration of the interval shown is ≤ 1 m.y.

The excursion is thereby magnified in the organic material, with a total magnitude of $\sim -1.5‰$. This isotopic signature of decreased silicate weathering (Fig. 12b) is thus virtually indistinguishable from that of increased volcanism (Fig. 11a). Interestingly, the Sr isotopic response to these two perturbations (decreased silicate weathering delivery of radiogenic Sr or increased submarine volcanism and hydrothermal influx of non-radiogenic Sr) would also be difficult to distinguish, so combining isotopic data for carbon and strontium does not solve the underdetermined nature of the problem (e.g., Kump, 1989).

Rather than look for an example of this sort of behavior in the isotopic record, we build on the complexity of the response by considering the consequences of simultaneous reductions in both silicate and organic-carbon weathering rates.

3.1.7. Model-data comparison III: Late Ordovician isotopic excursion

Organic carbon is most abundant in fine-grained terrigenous rocks (shales), which otherwise are considered 'silicate' rocks in the context of the carbonate/silicate cycle. Because of the restriction of shelf carbonate deposition to low latitudes, there is a tendency for carbonate lithologies to be exposed preferentially at low latitudes and silicates (by default) at high latitudes. One interesting consequence of this is that a glacioeustatic sea-level fall, caused by ice-sheet growth on high-latitude continents, could expose carbonates to weathering processes at low latitudes (where chemical weathering tends to be intense) while covering up silicate-weathering terrains at high latitudes (Gibbs and Kump, 1994). Such an explanation has been put forth by Kump et al. (in press) for the Late Ordovician glaciation and its isotopic response (Fig. 13).

A plausible scenario for the Late Ordovician glaciation is a total cessation in silicate weathering coupled to a 50% decrease in organic carbon weathering because of ice-sheet coverage at high latitudes (Fig. 14a). Total weathering rates may not have diminished because of exposure of carbonate platforms dominating low-latitudes, implying that carbonate weathering increased slightly (from $34{,}000 \times 10^{12}$ mol/ky to $39{,}000 \times 10^{12}$ mol/ky). Under these conditions both δ_{carb} and δ_{org} increase by approximately 2‰ (Fig. 14b). (The Late Ordovician excursion is considerably larger, implying a more dramatic change than explored here.) Interestingly, atmospheric pCO_2 rises during the perturbation because of the reduction in silicate weathering rate. This rise could be the mechanism of termination for the glaciation (Kump et al., in press).

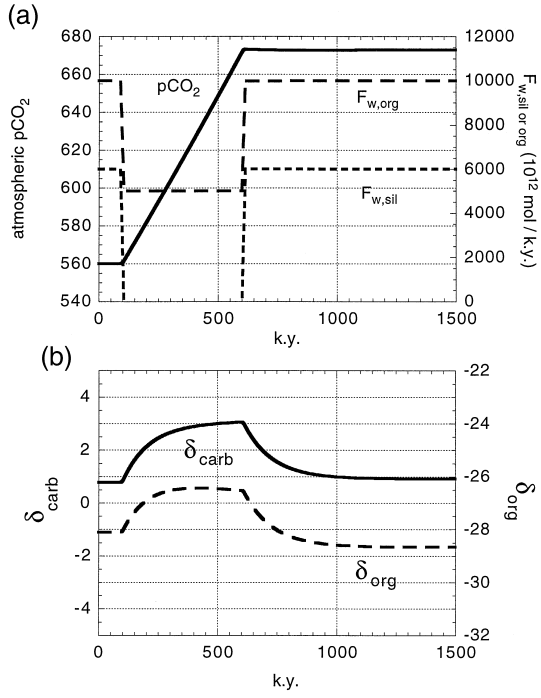

Fig. 14. The response of (a) atmospheric pCO_2 and (b) the inorganic- and organic-carbon isotopic composition of marine sediments to a 50% reduction in organic carbon weathering and a total cessation of silicate weathering, applied for 500 ky.

3.1.8. Perturbation 4: effect of C_4 plants

The isotopic composition of terrestrial organic matter preserved in paleosols underwent a substantial enrichment during the interval 8–6 Ma, reflecting the spread of C_4 grasses. (e.g., Quade et al., 1989). The cause of this expansion likely is the combination of a global reduction in atmospheric pCO_2, which would favor C_4 plants with relatively low CO_2 compensation points (e.g., Cerling, 1997; Tolbert et al., 1995), and increased aridity developed at various times at various places (e.g., Ruddiman et al., 1997). The C_4 photosynthetic pathway is associated with a much reduced isotopic discrimination for ^{12}C, and thus the burial of a substantial amount of C_4 plant-derived organic matter should affect Δ_B.

Derry and France-Lanord (1996) estimated that today, marine organic matter has an isotopic composition $\delta_{org,m} = -21‰$, while terrestrial C_3 organic matter has $\delta_{org,t3} = -28‰$, and terrestrial C_4 organic matter has $\delta_{org,t4} = -12‰$. Using these values, the relative proportions of terrestrial (X_{t3}) and marine (X_m) burial of organic matter before the spread of C_4 plants in the Late Miocene, indicated by our initial, steady-state model is given by:

$$\Delta_B = X_{t3}\delta_{org,t3} + X_m\delta_{org,m} \quad (15)$$

or

$$X_{t3} = \frac{\Delta_B - \delta_{org,m}}{\delta_{org,t3} - \delta_{org,m}} \quad (16)$$

which for the values given above gives $X_{t3} \sim 0.5$. This proportion is not unreasonable given the uncertainties of various estimates of the proportion of terrestrial organic carbon burial (Berner, 1982; Ittekot, 1988; Hedges and Keil, 1995).

We cannot uniquely determine these proportions after the rise of C_4 plants, but if the ratio of C_4 to C_3 burial of terrestrial organic matter were 1:1, then the isotopic composition of the terrestrial source would be virtually the same as the marine source, and Δ_B would be about $-20‰$. In our model, the resulting 5‰ decrease in Δ_B drives a 1‰ negative excursion in δ_{carb} (Fig. 15), and the approach to a new steady state takes about 200 ky. Once the perturbation is removed, all values return to their initial states because atmospheric pCO_2 has not responded to this change in the isotopic composition of the global burial flux of organic carbon.

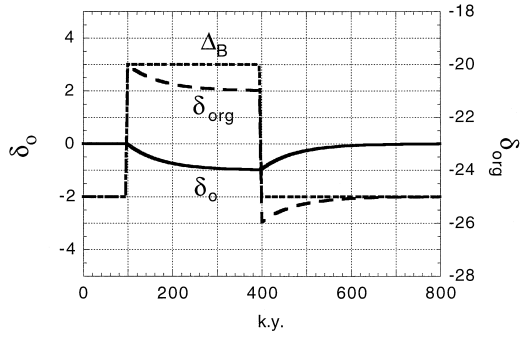

Fig. 15. The response of the inorganic- and organic-carbon isotopic composition to a change in Δ_B caused by a change in the isotopic composition of the source material. In this case Δ_B decreases (in absolute value) for 300 ky, in response, for example, to a shift toward a significant C_4 vegetation contribution to organic carbon burial. The δ_{org} curve tracks the response of the autochthonous marine organic carbon pool.

In reality, the expansion of C_4 grasses was more or less permanent, and thus so too should be its impact on the carbon isotopic composition of the ocean/atmosphere system. Perhaps the decrease in δ_{carb} noted by Shackleton (1985) for the late Neogene is a reflection of this phenomenon (Kump, 1989). The permanence of the effect, though, presumes that the falling atmospheric pCO_2 of the late Cenozoic was the driver for this ecological shift. Even if so, the global fossil-fuel burning experiment we are conducting may ultimately create conditions more similar to the early Tertiary or Cretaceous, when there was little competitive advantage for C_4 over C_3 plants.

4. Conclusions

Consideration of the isotopic mass-balance constraints imposed on the ocean-atmosphere system, together with the proposed sensitivity of the isotopic composition of organic matter to changes in atmospheric pCO_2, has led to the following conclusions.

(1) Increased burial of organic carbon leads to a fall in atmospheric pCO_2, and a positive excursions in both inorganic and organic carbon. The peak in organic carbon $\delta^{13}C$ may post-date that of inorganic carbon and may be larger in magnitude, because Δ_B

decreases as atmospheric pCO_2 falls. This difference in response is tied to a drawdown in atmospheric pCO_2. If the perturbation is fairly long-lived ($> 10^5$ years), the overall shift in $\delta^{13}C$ of carbonates may actually reverse, belying the continued elevated rates of organic carbon burial. Moreover, if the burial event is the result of an increase in riverine P supply, the associated pulse of isotopically light riverine carbon can cause a temporary negative shift in the carbon isotopic composition of the ocean/atmosphere reservoir. A reduction in organic carbon weathering causes an identical response.

(2) Increased volcanism leads to only small changes in the inorganic carbon isotopic composition of the ocean and limestones deposited from it, but can drive per mil variations in the isotopic composition of organic matter, because of the increase in magnitude of Δ_B.

(3) Decreased silicate weathering causes isotopic responses similar to those of increased volcanism, but only if the associated drawdown in atmospheric pCO_2 affects the photosynthetic isotopic effect.

(4) An increase in the proportion of carbonate weathering, relative to organic carbon and silicate weathering, can drive a large, positive excursion in the isotopic composition of the ocean.

(5) A significant change in the isotopic composition of terrestrial vegetation, resulting, for example, from an increase in the proportion of C_4 plant-derived organic matter, should be reflected in the oceanic organic isotopic compositions. The rise of C_4 plants should have caused a negative excursion in the ocean's isotopic composition and a positive excursion in the carbon isotopic composition of sedimentary organic matter.

References

Arthur, M.A., Sageman, B.B., 1994. Marine black shales: a review of depositional mechanisms and significance of ancient deposits. Annu. Rev. Earth Planet. Sci. 22, 499–551.

Arthur, M.A., Dean, W.E., Claypool, G.E., 1985. Anomalous ^{13}C enrichment in modern marine organic carbon. Nature 315, 216–218.

Arthur, M.A., Schlanger, S.O, Jenkyns, H.C., 1987. The Cenomanian–Turonian oceanic anoxic event: II. Paleoceanographic controls on organic matter production and preservation. In: Brooks, J., Fleet, A. (Eds.), Marine Petroleum Source Rocks. Geological Society of London, UK, pp. 401–420.

Arthur, M.A., Dean, W.E., Pratt, L.M., 1988. Geochemical and climatic effects of increased marine organic carbon burial at the Cenomanian/Turonian boundary. Nature 335, 714–717.

Berner, R.A., 1982. Burial of organic carbon and pyrite sulfur in the modern ocean: its geochemical and environmental significance. Am. J. Sci. 282, 451–473.

Berner, R.A., 1994. GEOCARB II: a revised model of atmospheric CO_2 over Phanerozoic time. Am. J. Sci. 294, 56–91.

Berner, R.A., Lasaga, A.C., Garrels, R.M., 1983. The carbonate–silicate geochemical cycle and its effect on atmospheric carbon dioxide over the last 100 million years. Am. J. Sci. 283, 641–683.

Bidigare, R.R. et al., 1997. Consistent fractionation of ^{13}C in nature and in the laboratory: growth-rate effects in some haptophyte algae. Global Biogeochem. Cycles 11, 279–292.

Bluth, G.J.S., Kump, L.R., 1991. Phanerozoic paleogeology. Am. J. Sci. 291, 284–308.

Bralower, T.J., Thierstein, H.R., 1984. Low productivity and slow deep-water circulation in mid-Cretaceous oceans. Geology 12, 614–618.

Brenchley, P.J., Carden, G.A.F., Marshall, J.D., 1995. Environmental changes associated with the 'first strike' of the Late Ordovician mass extinction. Mod. Geol. 20, 69–82.

Broecker, W.S., Peng, T.H., 1982. Tracers in the Sea. Lamont-Doherty Geol. Obs., Palisades, NY.

Broecker, W.S., Peng, T.H., 1987. The role of $CaCO_3$ compensation in the glacial to interglacial atmospheric CO_2 change. Global Biogeochem. Cycles 3, 215–239.

Cerling, T., 1997. Late Cenozoic vegetation change, atmospheric CO_2, and tectonics. In: Ruddiman, W.F. (Ed.), Tectonic Uplift and Climate Change. Plenum, New York, pp. 313–327.

Dean, E.D., Arthur, M.A., Claypool, G.E., 1986. Depletion of ^{13}C in Cretaceous marine organic matter: source, diagenetic, or environmental signal?. Mar. Geol. 7, 119–157.

Deines, P., 1980. The isotopic composition of reduced organic carbon. In: Fritz, P., Fontes, J.C. (Eds.), Handbook of Environmental Isotope Geochemistry, Vol. 1. Elsevier, Amsterdam, pp. 329–406.

Derry, L.A., France-Lanord, C., 1996. Neogene growth of the sedimentary organic carbon reservoir. Paleoceanography 11, 267–275.

Fischer, A.G., 1982. Long-term climatic oscillations recorded in stratigraphy. In: Climate in Earth History. National Academy of Sciences, Washington, DC, pp. 97–104.

Freeman, K.H., Hayes, J.M., 1992. Fractionation of carbon isotopes by phytoplankton and estimates of ancient pCO_2 levels. Global Biogeochem. Cycles 6, 629–644.

Garrels, R.M., Lerman, A., 1981. Phanerozoic cycles of sedimentary carbon and sulfur. Proc. Natl. Acad. Sci. U.S.A. 78, 4652–4656.

Garrels, R.M., Lerman, A., 1984. Coupling of the sedimentary sulfur and carbon cycles — an improved model. Am. J. Sci. 284, 989–1007.

Gibbs, M.T., Kump, L.R., 1994. Global chemical weathering at

the last glacial maximum and the present: sensitivity to changes in lithology and hydrology. Paleoceanography 9, 529–543.

Grotzinger, J.P., Knoll, A.H., 1995. Anomalous carbonate precipitates: is the Precambrian the key to the Permian?. Palaios 10, 578–596.

Hayes, J.M., Strauss, H., Kaufman, A.J., this volume. The abundance of ^{13}C in marine organic matter and isotopic fractionation in the global biogeochemical cycle of carbon during the past 800 Ma. Chem. Geol.

Hayes, J.M., Popp, B.N., Takigiku, R., Johnson, M.W., 1989. An isotopic study of biogeochemical relationships between carbonates and organic carbon in the Greenhorn Formation. Geochim. Cosmochim. Acta 53, 2961–2972.

Hedges, J.I., Keil, R.G., 1995. Sedimentary organic matter preservation: an assessment and speculative synthesis. Mar. Chem. 49, 81–115.

Hinga, K.R., Arthur, M.A., Pilson, M.E.Q., Whitaker, D., 1994. Carbon isotope fractionation by marine phytoplankton in culture: the effects of CO_2 concentration, pH, temperature, and species. Global Biogeochem. Cycles 8, 91–102.

Holland, H.D., 1984. The Chemical Evolution of the Atmosphere and Oceans. Princeton Univ. Press, NJ.

Hollander, D.J., McKenzie, J.A., 1991. CO_2 control on carbon-isotope fractionation during aqueous photosynthesis: a paleo-pCO_2 barometer. Geology 19, 929–932.

Holser, W.T., 1984. Gradual and abrupt shifts in ocean chemistry during Phanerozoic time. In: Holland, H.D., Trendall, A.F. (Eds.), Patterns of Change in Earth Evolution. Springer, Berlin, pp. 123–143.

Holser, W.T., Schidlowski, M., Mackenzie, F.T., Maynard, J.B., 1988. Biogeochemical cycles of carbon and sulfur. In: Gregor, C.B., Garrels, R.M., Mackenzie, F.T., Maynard, J.B. (Eds.), Chemical Cycles in the Evolution of the Earth. Wiley, New York, p. 105.

Ittekot, V., 1988. Global trends in the nature of organic matter in river suspensions. Nature 332, 436–438.

Jasper, J.P., Hayes, J.M., 1990. A carbon isotope record of CO_2 levels during the late Quaternary. Nature 347, 462–464.

Jasper, J.P., Hayes, J.M., Mix, A.C., Prahl, F.G., 1994. Photosynthetic frationation of ^{13}C and concentrations of dissolved CO_2 in the central equatorial Pacific during the last 255,000 years. Paleoceanography 9, 781–798.

Joachimski, M.M., 1997. Comparison of organic and inorganic carbon isotope patterns across the Frasnian–Famennian boundary. Palaeogeogr. Palaeoclim. Palaeoecol. 132, 133–145.

Keith, M.L., Weber, J.N., 1964. Carbon and oxygen isotopic composition of selected limestones and fossils. Geochim. Cosmochim. Acta 28, 1787–1816.

Kump, L.R., 1989. Alternative modeling approaches to the geochemical cycles of carbon, sulfur, and strontium isotopes. Am. J. Sci. 289, 390–410.

Kump, L.R., 1991. Interpreting carbon-isotope excursions: strangelove oceans. Geology 19, 299–302.

Kump, L.R., 1993, The coupling of the carbon and sulfur biogeochemical cycles over Phanerozoic time. In: Wollast, R., Mackenzie, F.T., Chou, L. (Eds.), Interactions of C, N, P and S Biogeochemical Cycles. Springer, Berlin, pp. 475–490.

Kump, L.R., Arthur, M.A., 1997. Global chemical erosion during the Cenozoic: Weatherability balances the budget. In: Ruddiman, W. (Ed.), Tectonic Uplift and Climate Change. Plenum, New York, pp. 399–426.

Kump, L.R., Garrels, R.M., 1986. Modeling atmospheric O_2 in the global sedimentary redox cycle. Am. J. Sci. 286, 337–360.

Kump, L.R., Gibbs, M.T., Arthur, M.A., Patzkowsky, M.E., Sheehan, P.M., 1995. Hirnantian glaciation and the carbon cycle. In: Cooper, J.D. et al. (Eds.), Ordovician Odyssey: Short Papers for the Seventh International Symposium on the Ordovician System. Pacific Section, Society for Sedimentary Geology, Fullerton, CA, pp. 299–302.

Kump, L.R., Arthur, M.A., Patzkowsky, M.E., Gibbs, M.T., Pinkus, D.S., Sheehan, P.M., in press. A weathering hypothesis for glaciation at high atmospheric pCO2 during the Late Ordovician. Palaeogeogr. Palaeoclimatol. Palaeoecol.

Laws, E.A., Popp, B.N., Bidigare, R.R., Kennicutt, M.C., Macko, S.A., 1995. Dependence of phytoplankton carbon isotopic composition on growth rate and $[CO_2]_{aq}$: theoretical considerations and experimental results. Geochim. Cosmochim. Acta 59, 1131–1135.

Lini, A., Weissert, H., Erba, E., 1992. The Valanginian carbon isotope event: a first episode of greenhouse climate during the Cretaceous. Terra Nova 4, 374–384.

Ludvigson, G.A., Jacobson, S.R., Witzke, B.J., Gonzalez, L.A., 1996. Carbonate component chemostratigraphy and depositional history of the Rocklandian Decorah Formation, Upper Mississippi Valley. In: Witzke, B.J. et al. (Eds.), Paleozoic Sequence Stratigraphy: View from the North American Craton. Geol. Soc. Am. Spec. Paper 306, Boulder, CO, pp. 67–86.

Magaritz, M., Krishnamurthy, R.V., Holser, W.T., 1992. Parallel trends in organic inorganic carbon isotopes across the Permian/Triassic boundary. Am. J. Sci. 292, 721–739.

Maslin, M.A., Hall, M.A., Shackleton, N.J., Thomas, E., 1996. Calculating surface water pCO_2 from foraminiferal organic $\delta^{13}C$. Geochim. Cosmochim. Acta 60 (24), 5089–5100.

Pagani, M., Arthur, M.A., Freeman, K.H., in review. Miocene evolution of atmospheric carbon dioxide. Paleoceanography, 1998.

Patzkowski, M.E., Slupik, L.M., Arthur, M.A., Pancost, R.D., Freeman, K.H., 1997. Late Middle Ordovician environmental change and extinction: Harbinger of the Late Ordovician or continuation of Cambrian patterns?. Geology 25, 911–914.

Popp, B.N., Takigiku, R., Hayes, J.M., Louda, J.W., Baker, E.W., 1989. The post-Paleozoic chronology and mechanism of ^{13}C depletion in primary marine organic matter. Am. J. Sci. 289, 436–454.

Pratt, L.M., Arthur, M.A., Dean, W.E., Scholle, P.A., 1993. Paleo-oceanographic cycles and events during the Late Cretaceous in the Western Interior Seaway of North America. In: Caldwell, W.G.E., Kauffman, E.G. (Eds.), Evolution of the Western Interior Basin. Geological Association of Canada Special Paper 39, pp. 333–353.

Quade, J., Cerling, T.E., Bowman, J.R., 1989. Development of Asian monsoon revealed by marked ecological shift during the latest Miocene in northern Pakistan. Nature 342, 163–166.

Rau, G.H., Takahashi, T., Des Marais, D.J., 1989. Latitudinal variations in plankton $\delta^{13}C$: implications for CO_2 and productivity in past oceans. Nature 341, 516–518.

Rau, G.H., Takahaski, T., Des Marais, D.J., Repeta, D.J., Martin, J.H., 1992. The relationship between $\delta^{13}C$ of organic matter and $[CO_{2,aq}]$ in ocean surface water: Data from a JGOFS site in the northeast Atlantic Ocean and a model. Geochim. Cosmochim. Acta 56, 1413–1419.

Rau, G.H., Riebesell, U., Wolf-Gladrow, D., 1997. $CO_{2,aq}$-dependent photosynthetic ^{13}C fractionation in the ocean: A model versus measurements. Global Biogeochem. Cycles 11, 267–278.

Raymo, M.E., Ruddiman, W.F., 1992. Tectonic forcing of late Cenozoic climate. Nature 359, 117–122.

Ruddiman, W.F., Kutzbach, J.E., Prentice, I.C., 1997. Testing the climatic effects of orography and CO_2 with general circulation and biome models. In: Ruddiman, W.F. (Ed.), Tectonic Uplift and Climate Change. Plenum, New York, pp. 203–235.

Schidlowski, M., Eichmann, R., Junge, C.E., 1975. Precambrian sedimentary carbonates: carbon and oxygen isotope geochemistry and implications for the terrestrial oxygen budget. Precambrian Res. 2, 1–69.

Scholle, P.A., Arthur, M.A., 1980. Carbon isotopic fluctuations in Cretaceous pelagic limestones — potential stratigraphic and petroleum exploration tool. Am. Assoc. Petrol. Geol. Bull. 64, 67–87.

Shackleton, N.J., 1985. Oceanic carbon isotope constraints on oxygen and carbon dioxide in the Cenozoic atmosphere. In: Sundquist, E., Broecker, W.S. (Eds.), The Carbon Cycle and Atmospheric CO_2: Natural Variations Archean to Present. Am. Geophys. Union, Washington, DC, pp. 412–417.

Stallard, R.F., Edmond, J.G., 1983. Geochemistry of the Amazon: 2. The influence of geology and weathering environment on the dissolved load. J. Geophys. Res. 88, 9671–9688.

Tolbert, N.E., Benker, C., Beck, E., 1995. The oxygen and carbon dioxide compensation points of C_3 plants: possible role in regulating atmospheric oxygen. Proc. Natl. Acad. Sci. U.S.A. 92, 11230–11233.

Veizer, J., Hoefs, J., 1976. The nature of O^{18}/O^{16} and C^{13}/C^{12} secular trends in sedimentary carbonate rocks. Geochim. Cosmochim. Acta 40, 1387–1395.

Zachos, J.C., Arthur, M.A., Dean, W.E., 1989. Geochemical evidence for suppression of pelagic marine productivity at the Cretaceous/Tertiary boundary. Nature 337, 61–64.